

# Electrochemical Performance of SnO<sub>2</sub> and SnO<sub>2</sub>/MWCNT/Graphene Composite Anodes for Li-Ion Batteries

O. CEVHER\* AND H. AKBULUT

Sakarya University, Engineering Faculty, Department of Metallurgical and Material Engineering, Esentepe Campus, 54187 Sakarya, Turkey

In this study, tin oxide (SnO<sub>2</sub>) coatings on Cr coated stainless steel and multi-walled carbon nanotube (MWCNT)/graphene substrates were prepared using a radio frequency magnetron sputtering process as anode materials in lithium-ion batteries. SnO<sub>2</sub> thin film and SnO<sub>2</sub>/MWCNT/graphene composite were characterized with field-emission scanning electron microscopy, X-ray diffraction, and electrochemical tests (cyclic voltammetry and galvanostatic cycling). The electrochemical properties of SnO<sub>2</sub> and SnO<sub>2</sub>/MWCNT/graphene composite anodes were studied using 2016-type coin cells assembled in an argon-filled glove box. The cells were cyclically tested on a MTI BST8-MA battery analyzer. The cyclic voltammograms of SnO<sub>2</sub> anode and SnO<sub>2</sub>/MWCNT/graphene composite anode were obtained over the potential range of 0.05–3.0 V and 0.05–2.5 V at a scan rate of 0.05 mV s<sup>-1</sup>, respectively.

DOI: [10.12693/APhysPolA.131.204](https://doi.org/10.12693/APhysPolA.131.204)

PACS/topics: 61.72.uj, 81.15.Cd, 82.47.Aa

## 1. Introduction

Tin oxide is an attractive material as a potential substitute for the conventional graphite anode in lithium-ion batteries, because the theoretical capacity of SnO<sub>2</sub> (1494 mAh g<sup>-1</sup>) [1] has been estimated to be superior to that of graphite (372 mAh g<sup>-1</sup>) [2]. But, SnO<sub>2</sub> presents limitations as a negative electrode material due to volume change of approximately 300% during Li alloying and dealloying, which pulverizes the electrode [3].

Graphene is one of the building blocks of all kinds of carbonaceous materials. A monolayer graphene sheet can be spirally wrapped into a single wall carbon nanotube. Multiple graphene sheets can be stacked into graphite with multi-layered graphene sheets which, in turn can be clustered into hard carbons or wrapped into multi-wall carbon nanotubes. Therefore, graphene structure provides an ideal platform for fundamental understanding of Li-C [4].

Owing to its vast surface-to-volume ratio and highly conductive nature, graphene may also bring high Li storage capacity to Li-ion batteries [5, 6].

In this study, it is aimed to produce a modified lithium ion battery electrode consisting of SnO<sub>2</sub> nanocrystals on the surface of MWCNT/graphene paper. Since one of the main problems of the SnO<sub>2</sub> based anode electrodes is the poor electronic conductivity, MWCNT/graphene was selected as substrate material. In addition, the larger surface areas of these electrode materials lower the local current density, resulting in a decrease of concentration polarization. Moreover, it is well-known that increase of the electrochemical performances of the metal oxide

anodes can be achieved by producing nanosized grains, thin films, mesoporous structures and nanocomposites, containing buffer components. Here we report SnO<sub>2</sub> thin films with nanostructured grains as negative electrodes for lithium ion batteries. The SnO<sub>2</sub> thin film was deposited onto MWCNT/graphene paper substrate by a magnetron sputtering process. SnO<sub>2</sub> thin films for lithium ion batteries were deposited using magnetron sputtering techniques in order to obtain mechanically strong and electrochemically stable and highly reversible anode electrodes.

## 2. Materials and methods

Graphene was obtained from flake graphite using the method described by Hummers [7]. MWCNT's (production by scalable chemical vapor deposition (CVD) method, purity: MWCNT's > 95%, diameter > 50 nm, length > 5 mm) were purchased from Aray International Group Limited (Germany). In our previous study, we have described chemically functionalization process of the MWCNT [8]. Flexible MWCNT/graphene paper was prepared by vacuum filtration method. MWCNT (20 mg) and graphene (20 mg) was dispersed with 200 mg of sodium dodecyl sulfate (SDS) in 100 ml of deionized water and sonicated for 1 h. PVDF membranes with a pore size of 220 nm were used in vacuum filtration. Then, flexible MWCNT/graphene paper was separated from the PVDF membrane, further compacted and dried at 40 °C for 24 h. The average thickness of the produced MWCNT/graphene paper is approximately 100 μm and their diameter was about 16 mm.

SnO<sub>2</sub> films were deposited by RF magnetron sputtering on MWCNT/graphene paper and Cr coated stainless steel substrates. The target was a SnO<sub>2</sub> disc (SnO<sub>2</sub> 99.9% pure, Kurt J. Lesker Company) with a diameter of 50.8 mm and 3.17 mm thick. SnO<sub>2</sub> films were deposited at a pressure of 1.0 Pa with a RF power of 100 W

\*corresponding author; e-mail: [ocevher@sakarya.edu.tr](mailto:ocevher@sakarya.edu.tr)

in O<sub>2</sub>/Ar (5/95) gas mixture. The distance between target and substrate was about 13.5 cm. The flow rate of O<sub>2</sub>/Ar gas mixture was fixed by a TDZM-III mass flow controller.

The surface morphologies of SnO<sub>2</sub> and SnO<sub>2</sub>/MWCNT/graphene composite were examined by field emission scanning electron microscopy (FESEM). X-ray diffraction (XRD) patterns of SnO<sub>2</sub> and SnO<sub>2</sub>/MWCNT/graphene composite samples were obtained via a X-ray diffractometer (Rigaku D/MAX 2000 with a multipurpose attachment) using Cu K<sub>α</sub> radiation ( $\lambda = 1.54056 \text{ \AA}$ ) in the  $2\theta$  diffraction range extending from 10 to 90°.

The electrochemical properties of SnO<sub>2</sub> anode and SnO<sub>2</sub>/MWCNT/graphene composite anode were studied using 2016-type coin cells assembled in an argon-filled glove box. The charge/discharge behavior of SnO<sub>2</sub> anode was measured galvanostatically at a charge/discharge rate of 1 C in the 0.05–3.0 V range and the charge/discharge behavior of SnO<sub>2</sub>/MWCNT/graphene composite anode was measured galvanostatically at a charge/discharge rate of 1 C in the 0.05–2.5 V range. One molar LiPF<sub>6</sub> in ethyl carbonate (EC) and dimethyl carbonate (DMC) (EC:DMC = 1:1 by volume) was used as the electrolyte. Cyclic voltammograms (CV) of SnO<sub>2</sub> anode and SnO<sub>2</sub>/MWCNT/graphene composite anode were measured on a Gamry Model 3000 electrochemical analyzer at a scan rate of 0.1 mV s<sup>-1</sup> between 0.05 and 3.0 V, and between 0.05 and 2.5 V versus Li<sup>+</sup>/Li, respectively.

### 3. Results and discussions

The FESEM morphology of SnO<sub>2</sub> film produced at 5% O<sub>2</sub> partial pressure on Cr coating the stainless steel substrate is presented in Fig. 1a. SnO<sub>2</sub> film has a relatively smooth and dense surface. Grain agglomerates are also observed. The results show that SnO<sub>2</sub> film is made of nanosized particles. FESEM images showing top views of the SnO<sub>2</sub>/MWCNT/graphene are presented in Fig. 1b. The film surface consists of randomly oriented entanglements of MWCNT/graphene composite. In addition, it is clear that MWCNT/graphene composite paper are porous, forming a random heavily interconnected network having a broad distribution of pore sizes.

The X-ray diffraction (XRD) patterns of SnO<sub>2</sub> film and SnO<sub>2</sub>/MWCNT/graphene composite are shown in Fig. 2. The diffraction angles at 26.3°, 33.6°, and 51.8°

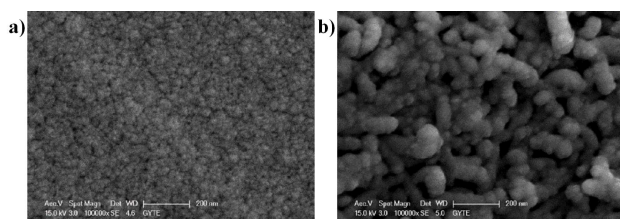


Fig. 1. Surface FESEM images: (a) SnO<sub>2</sub> film, (b) SnO<sub>2</sub>/MWCNT/graphene composite.

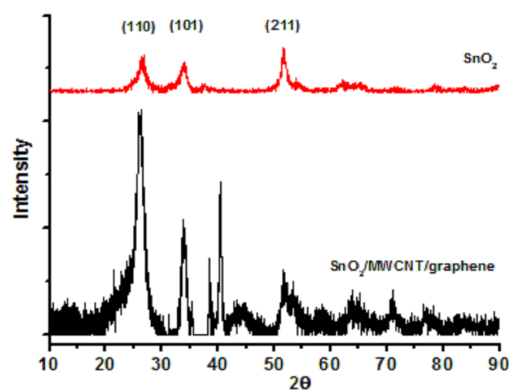


Fig. 2. The X-ray diffraction patterns of SnO<sub>2</sub> film and SnO<sub>2</sub>/MWCNT/graphene composite.

can be assigned to (110), (101) and (211) planes of the cassiterite structure of SnO<sub>2</sub>, respectively (JCPDS card 00-041-1445), and the characteristic peaks of the (002) and (101) reflections are observed at about 26° and 43° for the MWCNT, corresponding to JCPDS card 00-041-1487. The broad peak at around 25° is observed, which corresponds to the (002) plane of graphene sheets.

Figure 3a shows the first three CV of SnO<sub>2</sub> anode. The strong reduction peak appears at 0.85 V, which can be attributed to the irreversible reactions which form solid–electrolyte interphase (SEI). This peak does not appear in the subsequent voltammetric cycles. Two peaks at about 0.53 and 1.12 V appear in the anodic sweep process. The peak at 0.53 V represents the dealloying process of Li<sup>+</sup> ions [9, 10]. Figure 3b shows the first three CV of SnO<sub>2</sub>/MWCNT/graphene composite anode at 0.5 mV/s. As can be seen from Fig. 3b, during the first cathodic potential sweeping, a reduction peak appears at 0.58 V, which can be attributed to the irreversible reactions which form surface films. This peak does not appear in the subsequent voltammetric cycles. Hence, the first CV cycle can be considered as a formation cycle, and then the electrode demonstrates quite a reversible behavior. The cathodic peak between 0.1 V and 0.3 V can be attributed to the process of alloying of tin with lithium [11, 12].

The discharge–charge curves of SnO<sub>2</sub> anode materials during the 50th cycle at a constant current of 1.0 C shown in Fig. 4a. As shown in Fig. 4a, the discharge and charge capacities of the 1st cycle are 1587 mAh g<sup>-1</sup> and 963 mAh g<sup>-1</sup>, respectively. As can be seen from Fig. 4a, the discharge capacity of SnO<sub>2</sub> anode material at the 50th cycle is approximately 63 mAh g<sup>-1</sup>. The discharge–charge curves of SnO<sub>2</sub>/MWCNT/graphene composite anode materials during the 100th cycle at a constant current of 1.0 C shown in Fig. 4b. As shown in Fig. 4b, the discharge and charge capacities of the 1st cycle are 1676 mAh g<sup>-1</sup> and 1125 mAh g<sup>-1</sup>, respectively. As can be seen from Fig. 4b, the discharge capacity of SnO<sub>2</sub>/MWCNT/graphene composite anode material at the 100th cycle is approximately 885 mAh g<sup>-1</sup>.

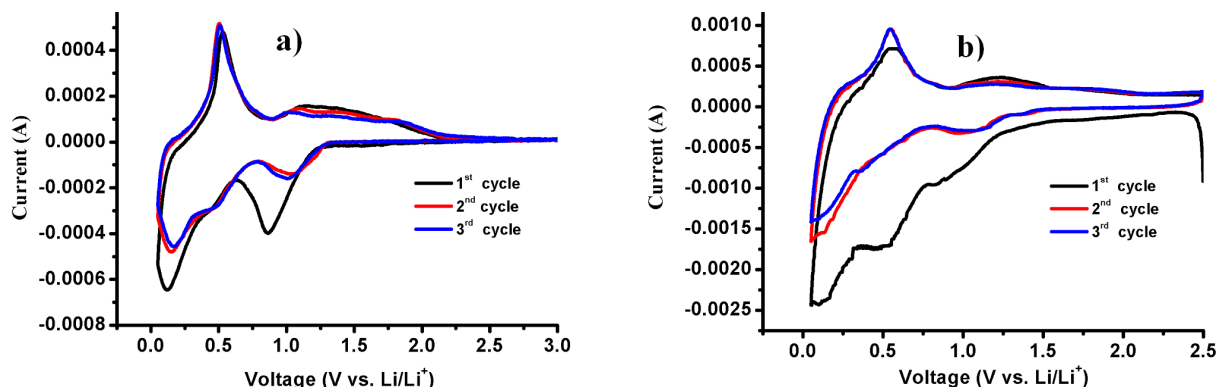


Fig. 3. The cyclic voltammograms of (a)  $\text{SnO}_2$  anode and (b)  $\text{SnO}_2/\text{MWCNT}/\text{graphene}$  composite anode.

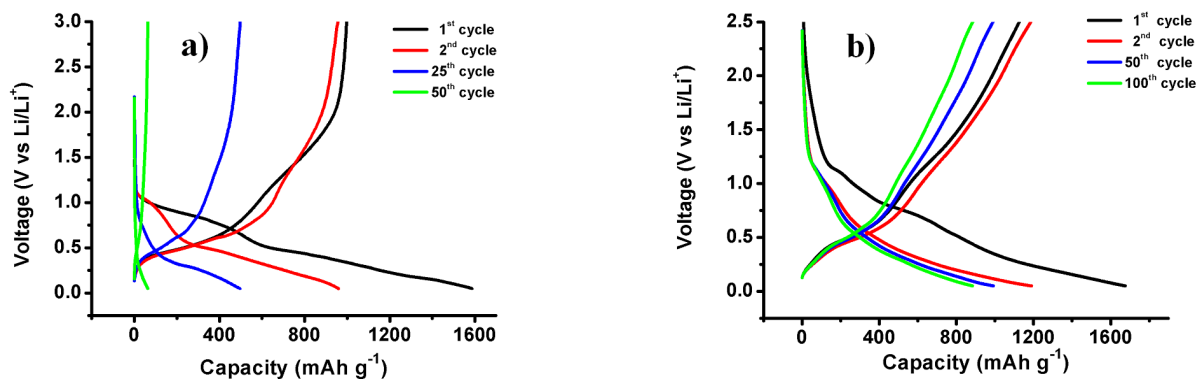


Fig. 4. The discharge/charge curves of anode materials: (a)  $\text{SnO}_2$  anode, (b)  $\text{SnO}_2/\text{MWCNT}/\text{graphene}$  composite anodes.

#### 4. Conclusion

$\text{SnO}_2$  coatings on Cr coated stainless steel and MWCNT/graphene substrates were prepared by the RF magnetron sputtering process. When used as anode materials for lithium-ion batteries, the  $\text{SnO}_2/\text{MWCNT}/\text{graphene}$  composite electrode exhibits better electrochemical performance than the pure  $\text{SnO}_2$ , which is mainly because the high surface area and porous structure of MWCNT/graphene paper can effectively accommodate the volume change during charge and discharge process. Thus MWCNT/graphene paper improves the stability and the cycle life of the anode in a lithium ion battery. These results show that  $\text{SnO}_2/\text{MWCNT}/\text{graphene}$  composite is promising anode materials for Li-ion battery applications.

#### References

- [1] N. Mohri, B. Oschmann, N. Laszczynski, F. Mueller, J. Zamory, M.N. Tahir, S. Passerini, R. Zentel, W. Tremel, *J. Mater. Chem. A* **4**, 612 (2016).
- [2] H. Liu, Z. Hu, R. Hu, H. Ruan, Y. Su, L. Zhang, *Int. J. Electrochem. Sci.* **11**, 3376 (2016).
- [3] J. Li, Y. Zhao, N. Wang, L. Guan, *Chem. Commun.* **47**, 5238 (2011).
- [4] N. Kheirabadi, A. Shafiekhani, *J. Appl. Phys.* **112**, 124323 (2012).
- [5] E.J. Yoo, J. Kim, E. Hosono, H.S. Zhou, T. Kudo, I. Honma, *Nano Lett.* **8**, 2277 (2008).
- [6] G. Wang, B. Wang, X. Wang, J. Park, S. Dou, H. Ahn, K. Kim, *J. Mater. Chem.* **19**, 8378 (2009).
- [7] T. Cetinkaya, M. Tokur, S. Ozcan, M. Uysal, H. Akbulut, *Int. J. Hydrogen Energy* **41**, 6945 (2016).
- [8] U. Tocoglu, M. Alaf, O. Cevher, M.O. Guler, H. Akbulut, *J. Nanosci. Nanotechnol.* **12**, 9169 (2012).
- [9] L. Zhao, L. Gao, *Carbon* **42**, 1858 (2004).
- [10] L. Noerochim, J.Z. Wang, S.L. Chou, H.J. Li, H.K. Liu, *Electrochim. Acta* **56**, 314 (2010).
- [11] J. Santos-Pena, T. Brousse, L. Sanchez, J. Morales, D.M. Schleich, *J. Power Sourc.* **97-98**, 232 (2001).
- [12] Y. Wang, T. Chen, *Electrochim. Acta* **54**, 3510 (2009).